Binary Association Complexes of LiH, BeH_2, and BH_3. Relative Isomer Stabilities and Barrier Heights for Their Interconversion: Energy Barriers in the Dimerization Reactions

D. J. DeFrees,*[1a] Krishnan Raghavachari,*[1b] H. B. Schlegel,*[1c] J. A. Pople,*[1d] and P. v. R. Schleyer*[1e]

Department of Chemistry, Carnegie-Mellon University, Pittsburgh, Pennsylvania 15213; Molecular Research Institute, Palo Alto, California 94304; AT&T Bell Laboratories, Murray Hill, New Jersey 07974; Department of Chemistry, Wayne State University, Detroit, Michigan 48202; and Institut für Organische Chemie, Universität Erlangen-Nürnberg, D-8520 Erlangen, Federal Republic of Germany
(Received: November 17, 1986)

Ab initio molecular orbital theory has been used to study the six compounds Li_2H_2, $LiBeH_3$, $LiBH_4$, Be_2H_4, $BeBH_5$, and B_2H_6. Geometry optimizations and vibrational analysis at the HF/6-31G* level indicate Li--$(H)_2$--Li (D_{2h}), Li--$(H)_2$--BeH (C_{2v}), Li--$(H)_3$--BH (C_{3v}), HBe--$(H)_2$--BeH (D_{2h}), HBe--$(H)_3$--BH (C_{3v}), and H_2B--$(H)_2$--BH_2 (D_{2h}) to be the most stable forms. Inclusion of electron correlation corrections at the MP4/6-31G** level does not alter these conclusions. Other isomers were also examined in detail, and it was found that the potential energy surfaces for the species are generally flat. Activation energies for isomer interconversion and hydrogen scrambling reactions are generally less than 10 kcal mol^{-1}. Examination of the HF/3-21G potential surfaces indicates that there is no activation energy for the dimerization of LiH or BeH_2. The same is true for the dimerization of BH_3 at the correlated MP2/6-31G* level, although a small barrier is found on the HF/6-31G* surface. Enthalpies of complexation at 298 K from separate LiH, BeH_2, and BH_3 fragments, $\Delta H°_{298}$, computed by using the HF/6-31G* harmonic frequencies and the MP4/6-31G** electronic energies are as follows: Li_2H_2, -45.9; $LiBeH_3$, -43.6; $LiBH_4$, -60.1; Be_2H_4, -30.5; $BeBH_5$, -45.7; B_2H_6, -36.0 kcal mol^{-1}.

Introduction

The electron-deficient hydrides of lithium (LiH), beryllium (BeH_2), and boron (BH_3) interact to form six binary association complexes which can contain a number of bridging hydrogen atoms.[2,3] Diborane, the experimentally well-established BH_3 dimer, has two such hydrogens.[3] LiH,[2,3] $LiBeH_3$,[4] and $LiBH_4$[2] are known as crystalline solids; the atomization energy of the lithium hydride dimer, $(LiH)_2$, has been determined experimentally.[5] Solid BeH_2 is throught to be a polymer with two bridging hydrogens between each pair of beryllium atoms.[2,6]

In an earlier ab initio molecular orbital study,[2] the relative energies of structures with various numbers of bridging hydrogens were considered, and it was concluded that the most stable forms were Li--$(H)_2$--Li (D_{2h}), Li--$(H)_2$--BeH (C_{2v}), Li--$(H)_3$--BH (C_{3v}), HBe--$(H)_2$--BeH (D_{2h}), HBe--$(H)_3$--BH (C_{3v}), and H_2B--$(H)_2$--BH_2 (D_{2h}, with bridging and terminal hydrogens in perpendicular planes). Some of these complexes can be considered to be ionic. For example, lithium borohydride can be viewed as a Li^+ cation attached to the face of a BH_4^- tetrahedron, Li--$(H)_3$--BH; structures with edge (Li--$(H)_2$--BH_2) or corner (Li--H--BH_3) attachments are less stable.

The previous study was carried out entirely at the Hartree–Fock (HF) level.[2] Geometries were optimized with the minimal STO-3G[7] basis set, and single-point computations were performed using the 6-31G* basis[8] (split-valence with polarization functions on non-hydrogen atoms). The results left a number of unanswered questions:

1. Are the results modified if a higher level basis is used for geometry optimization?
2. Does inclusion of polarization functions on hydrogen (p functions) change the relative energies of structures with different numbers of bridging atoms?
3. Do the stationary points found on the potential surface all correspond to local minima (separate isomers) or are some of them saddle points (transition structures connecting distinct isomers *or* connecting equivalent isomers) leading to scrambling of the bridging and terminal hydrogens?
4. Are the relative isomer energies and binding energies (for dissociation to separate LiH, BeH_2, and BH_3 fragments) altered significantly if electron correlation is included in the theoretical model?
5. What is the nature of the association reactions; are there activation barriers?

Since only partial answers to some of these questions can be found in the literature, much of which was cited in our previous paper,[2] or in recent studies (cited below), a comprehensive reexamination of these six compounds at a *uniform level of theory*

TABLE I: Distances (Å) between Non-Hydrogen Atoms

molecule	point group	STO-3G	3-21G	6-31G*
LiH--LiH	$C_{\infty v}$	3.331	3.445	3.436
Li--$(H)_2$--Li	D_{2h}	2.222	2.364	2.343
LiH--BeH_2	C_{2v}	3.122	3.123	3.104
Li--$(H)_2$--BeH	C_{2v}	2.157	2.284	2.243
Li--$(H)_3$--Be	C_{3v}	1.842	1.977	1.940
Li--$(H)_2$--BH_2	C_{2v}	2.083	2.193	2.154
Li--$(H)_3$--BH	C_{3v}	1.877	2.013	1.968
HBeH--BeH_2	C_{2v}	3.977	3.774	3.777
HBe--$(H)_2$--BeH	D_{2h}	1.991	2.050	2.018
HBe--$(H)_3$--Be	C_{3v}	1.738	1.803	1.774
HBeH--BH_3	C_{3v}	3.821	3.206	3.591
HBe--$(H)_2$-BH_2	C_{2v}	1.876	1.891	1.870
HBe--$(H)_3$--BH	C_{3v}	1.686	1.732	1.700
H_2B--$(H)_2$--BH_2	D_{2h}	1.805	1.785	1.778

(1) (a) Carnegie-Mellon University and Molecular Research Institute. Current address: Molecular Research Institute. (b) Carnegie-Mellon University and AT&T Bell Laboratories. Current address: AT&T Bell Laboratories. (c) Carnegie-Mellon University and Wayne State University. Current address: Wayne State University. (d) Carnegie-Mellon University. (e) Universität Erlangen-Nürnberg.

(2) Dill, J. D.; Schleyer, P. v. R.; Binkley, J. S.; Pople, J. A. *J. Am. Chem. Soc.* **1977**, *99*, 6159 and references cited therein.

(3) (a) Wiberg, E.; Amberger, E. *Hydrides of the Elements of Main Groups I-IV*; Elsevier: Amsterdam, 1971. (b) Wade, K. *Electron Deficient Compounds*; Nelson: 1971.

(4) Ashby, E. C.; Prasad, H. S. *Inorg. Chem.* **1975**, *14*, 2869.

(5) Ihle, H. R.; Wu, C. H. *Adv. Mass Spectrom.* **1978**, *7A*, 636.

(6) Marynick, D. S. *J. Am. Chem. Soc.* **1981**, *103*, 1328 and references cited therein.

(7) Hehre, W. J.; Stewart, R. F.; Pople, J. A. *J. Chem. Phys.* **1969**, *51*, 2657.

(8) Hariharan, P. C.; Pople, J. A. *Theor. Chim. Acta* **1973**, *28*, 213.

0022-3654/87/2091-1857$01.50/0

TABLE II: Optimized Total Energies (hartrees) and Number of Imaginary Frequencies[a]

molecule	point group	STO-3G	3-21G	6-31G*
LiH	$C_{\infty v}$	−7.863 38 (0)	−7.929 84 (0)	−7.980 87 (0)
BeH_2	$D_{\infty h}$	−15.561 35 (0)	−15.673 78 (0)	−15.765 93 (0)
BH_3	D_{3h}	−26.070 70 (0)	−26.237 30 (0)	−26.390 01 (0)
LiH--LiH	$C_{\infty v}$	−15.765 10 (2)	−15.902 19 (0)	−16.003 31 (0)
Li--$(H)_2$--Li	D_{2h}	−15.796 81 (0)	−15.933 25 (0)	−16.035 59 (0)
LiH--BeH_2	C_{2v}	−23.442 46 (2)	−23.634 38 (2)	−23.777 67 (2)
Li--$(H)_2$--BeH	C_{2v}	−23.481 86 (0)	−23.664 47 (0)	−23.811 00 (0)
Li--$(H)_3$--Be	C_{3v}	−23.458 04 (0)	−23.641 45 (0)	−23.788 85 (0)
Li--$(H)_2$--BH_2	C_{2v}	−33.992 07 (1)	−34.238 07 (1)	−34.441 92 (1)
Li--$(H)_3$--BH	C_{3v}	−34.002 47 (0)	−34.243 84 (0)	−34.449 98 (0)
HBeH--BeH_2	C_{2v}	−31.123 57 (0)	−31.349 44 (1)	−31.533 14 (1)
HBe--$(H)_2$--BeH	D_{2h}	−31.154 00 (0)	−31.378 05 (0)	−31.570 19 (0)
HBe--$(H)_3$--Be	C_{3v}	−31.108 96 (0)	−31.334 10 (0)	−31.527 86 (0)
HBeH--BH_3	C_{3v}	−41.633 03 (2)	−41.915 66 (0)	−42.157 91 (2)
HBe--$(H)_2$--BH_2	C_{2v}	−41.667 59 (0)	−41.949 45 (0)	−42.200 74 (0)
HBe--$(H)_3$--BH	C_{3v}	−41.669 87 (0)	−41.948 31 (0)	−42.205 28 (0)
H_2B--$(H)_2$--BH_2	D_{2h}	−52.166 10 (0)	−52.497 81 (0)	−52.812 40 (0)

[a] In parentheses following the total energy.

is appropriate. The objective of this paper is to examine these molecules by using newer theoretical methods in an attempt to answer the questions posed above.

Theoretical Methods and Results

The most favorable HF/STO-3G structures, reported previously,[2] were optimized by gradient minimization[9] within the indicated symmetry constraints using the split-valence 3-21G basis[10] and the polarization 6-31G* basis set.[8] Table I gives the distances between non-hydrogen atoms; full structures are published separately.[11] Addition of p polarization functions to the basis set used for geometry optimization (HF/6-31G** geometries) does not significantly alter the result. For example, the HF/6-31G* geometry for diborane is r(B–B) = 1.778 Å, r(B–H_b) = 1.316 Å, r(B–H) = 1.185 Å, and ∠(H–B–H) = 122.1° (H_b indicates the bridging hydrogen); this is virtually identical with the HF/6-31G** geometry of r(B–B) = 1.778 Å, r(B–H_b) = 1.317 Å, r(B–H) = 1.185 Å, and ∠(H–B–H) = 122.0°. This is consistent with the small effect of p polarization functions on energies (vide infra). The optimized total energies for all the structures are listed in Table II.

At the HF/STO-3G, HF/3-21G, and HF/6-31G* levels, analytical second derivatives of the energy with respect to all nuclear coordinates[12] were evaluated in order to characterize the stationary points on the potential energy surface. In Table II the number of imaginary frequencies derived from the second-derivative (force constant) matrix is given in parentheses following the energy. Local minima are indicated by a "(0)", saddle points by a "(1)", and double saddles by a "(2)". The HF/6-31G* frequencies and the corresponding zero-point vibrational energy for the most stable isomer of each of the six complexes are presented in Table III.

Using the HF/6-31G* geometries, single-point calculations were done with the 6-31G** basis set which also includes p polarization functions on hydrogen.[8] (These are denoted by HF/6-31G**//HF/6-31G*; the symbols after // indicate the level used for geometry optimization.) The effects of electron correlation were assessed by Møller–Plesset perturbation theory at second (MP2), third (MP3), and fourth (MP4) orders.[13] The complete

TABLE III: Harmonic Vibrational Frequencies (cm^{-1}) and Zero-Point Vibrational Energies (kcal mol^{-1}) Evaluated at the HF/6-31G* Level

molecule	point group	harmonic frequencies	ZPE
LiH	$C_{\infty v}$	1416(σ)	2.0
BeH_2	$D_{\infty h}$	761(π_u), 2107(σ_g), 2323(σ_u)	8.5
BH_3	D_{3h}	1225(a_2''), 1305(e'), 2693(a_1'), 2813(e')	17.4
Li--$(H)_2$--Li	D_{2h}	516(a_g), 609(b_{3u}), 851(b_{3g}), 952(b_{1u}), 1056(b_{2u}), 1164(a_g)	7.4
Li--$(H)_2$--BeH	C_{2v}	346(b_1), 589(a_1), 602(b_2), 899(b_1), 1137(b_2), 1259(a_1), 1517(b_2), 1663(a_1), 2085(a_1)	14.4
Li--$(H)_3$--BH	C_{3v}	491(e), 683(a_1), 1225(e), 1338(a_1), 1365(e), 2240(e), 2323(a_1), 2703(a_1)	25.3
HBe--$(H)_2$--BeH	D_{2h}	349(b_{3u}), 558(b_{2g}), 564(b_{3g}), 618(b_{2u}), 724(a_g), 989(b_{3u}), 1487(b_{3g}), 1561(b_{1u}), 1628(b_{2u}), 1834(a_g), 2197(b_{1u}), 2220(a_g)	21.1
HBe--$(H)_3$--BH	C_{3v}	550(e), 609(e), 936(a_1), 1262(e), 1454(e), 1497(a_1), 2234(a_1), 2324(e), 2371(a_1), 2865(a_1)	31.9
H_2B--$(H)_2$--BH_2	D_{2h}	409(b_{2u}), 828(a_g), 897(a_u), 900(b_{2g}), 999(b_{1g}), 1071(b_{1u}), 1127(b_{2u}), 1194(b_{3g}), 1286(b_{3u}), 1303(a_g), 1833(b_{3u}), 1932(b_{2g}), 2067(b_{1u}), 2300(a_g), 2734(b_{3u}), 2753(a_g), 2828(b_{1g}), 2842(b_{2u})	41.9

fourth-order treatment has contributions from single, double, triple, and quadruple substitutions from the reference Hartree–Fock determinent. Only the valence electron correlation was included in these calculations. The resulting total energies are listed in Table IV. The theoretical association energies are shown in Table V.

Internal energies, E, and third law entropies, S, were evaluated with the standard statistical mechanical formulas using the HF/6-31G* structures and normal-mode vibrational frequencies.[14] Computation of these thermochemical quantities at standard temperature (298.15 K) and pressure (1 atm) in the harmonic approximation assumed the separability of electronic, vibrational, rotational, and translational degrees of freedom. Quantities relating to the thermochemistry of the dimerization reactions are listed in Table VI.

The geometries of some of the isomers (vide infra) were also optimized at the MP2(Full)/6-31G* level of theory using analytical gradients of the energy with respect to the nuclear coordinates.[9,12a,15] The notation (Full) indicates that the correlation

(9) Schlegel, H. B. *J. Comput. Chem.* **1982**, *3*, 214.
(10) Binkley, J. S.; Pople, J. A.; Hehre, W. J. *J. Am. Chem. Soc.* **1980**, *102*, 939.
(11) Whiteside, R. A.; Frisch, M. J.; Binkley, J. S.; DeFrees, D. J.; Schlegel, H. B.; Raghavachari, K.; Pople, J. A. *Carnegie-Mellon Quantum Chemistry Archive*; Carnegie-Mellon University: Pittsburgh, PA, 1982.
(12) (a) Pople, J. A.; Krishnan, R.; Schlegel, H. B.; Binkley, J. S. *Int. J. Quantum Chem., Quantum Chem. Symp.* **1979**, *No. 13*, 225. (b) Pople, J. A.; Schlegel, H. B.; Krishnan, R.; DeFrees, D. J.; Binkely, J. S.; Frisch, M. J.; Whiteside, R. A.; Hout, R. F.; Hehre, W. J. *Int. J. Quantum Chem.* **1981**, *15*, 269.
(13) (a) Møller, C.; Plesset, M. S. *Phys. Rev.* **1934**, *46*, 618. (b) Krishnan, R.; Frisch, M. J.; Pople, J. A. *J. Chem. Phys.* **1980**, *72*, 4244 and references cited therein.
(14) McQuarrie, D. A. *Statistical Thermodynamics*; Harper and Row: New York, 1973; Chapter 8.

TABLE IV: Total Energies (hartrees) Calculated with the 6-31G Basis Set Using the 6-31G* Geometries**

molecule	point group	HF	MP2	MP3	MP4
LiH	$C_{\infty v}$	−7.981 34	−8.001 59	−8.006 18	−8.007 55
BeH_2	$D_{\infty h}$	−15.766 91	−15.815 71	−15.826 29	−15.829 07
BH_3	D_{3h}	−26.392 87	−26.486 15	−26.503 32	−26.507 54
LiH--LiH	$C_{\infty v}$	−16.003 72	−16.045 05	−16.054 24	−16.056 83
Li--$(H)_2$--Li	D_{2h}	−16.036 28	−16.079 26	−16.088 67	−16.091 23
LiH--BeH_2	C_{2v}	−23.778 62	−23.853 98	−23.869 43	−23.873 51
Li--$(H)_2$--BeH	C_{2v}	−23.812 62	−23.890 03	−23.905 91	−23.910 10
Li--$(H)_3$--Be	C_{3v}	−23.790 09	−23.870 52	−23.886 81	−23.891 13
Li--$(H)_2$--BH_2	C_{2v}	−34.445 92	−34.580 71	−34.601 41	−34.607 66
Li--$(H)_3$--BH	C_{3v}	−34.453 73	−34.590 56	−34.611 31	−34.617 57
HBeH--BeH_2	C_{2v}	−31.534 95	−31.633 86	−31.655 12	−31.660 70
HBe--$(H)_2$--BeH	D_{2h}	−31.572 56	−31.682 68	−31.705 07	−31.710 99
HBe--$(H)_3$--Be	C_{3v}	31.529 98	−31.647 22	−31.669 64	−31.675 92
HBeH--BH_3	C_{3v}	−42.161 58	−42.306 11	−42.333 84	−42.340 93
HBe--$(H)_2$--BH_2	C_{2v}	−42.205 70	−42.372 52	−42.399 77	−42.407 75
HBe--$(H)_3$--BH	C_{3v}	−42.210 09	−42.381 43	−42.408 23	−42.416 30
H_2B--$(H)_2$--BH_2	D_{2h}	−52.819 86	−53.038 34	−53.070 48	−53.080 40

TABLE V: Binding Energies (kcal mol^{-1}) Relative to LiH, BeH_2, and BH_3 Fragments[a] Calculated Using the 6-31G* Geometries

molecule	point group	6-31G* HF	6-31G** HF	6-31G** MP2	6-31G** MP3	6-31G** MP4
LiH--LiH	$C_{\infty v}$	26.1	25.8	26.3	26.3	26.2
Li--$(H)_2$--Li	D_{2h}	46.3	46.2	47.7	47.9	47.8
LiH--BeH_2	C_{2v}	19.4	19.1	23.0	23.2	23.1
Li--$(H)_2$--BeH	C_{2v}	40.3	40.4	45.6	46.1	46.1
Li--$(H)_3$--Be	C_{3v}	26.1	26.3	33.4	34.1	34.2
Li--$(H)_2$--BH_2	C_{2v}	44.6	45.0	58.3	57.7	58.1
Li--$(H)_3$--BH	C_{3v}	49.6	49.9	64.5	63.9	64.3
HBeH--BeH_2	C_{2v}	0.8	0.7	1.5	1.6	1.6
HBe--$(H)_2$-BeH	D_{2h}	24.1	24.3	32.2	32.9	33.2
HBe--$(H)_3$--Be	C_{3v}	−2.5	−2.4	9.9	10.7	11.2
HBeH--BH_3	C_{3v}	1.2	1.1	2.7	2.6	2.7
HBe--$(H)_2$--BH_2	C_{2v}	28.1	28.8	44.3	44.0	44.6
HBe--$(H)_3$--BH	C_{3v}	31.0	31.6	49.9	49.3	50.0
H_2B--$(H)_2$--BH_2	D_{2h}	20.3	21.4	41.4	40.1	41.0

[a] A negative sign indicates that the dimer is higher in energy than the separated monomers.

of all electrons was included in these calculations. The optimizations were followed by evaluation of the corresponding force constant matrices[16] by finite differencing of the analyical gradients.

Pathways for the dimerization reactions $2LiH \rightarrow Li_2H_2$, $2BeH_2 \rightarrow Be_2H_4$, and $2BH_3 \rightarrow B_2H_6$ were examined to determine whether any activation energy is required. The M–M distance (M being Li, Be, or B) was chosen as a reaction coordinate, R. For the first two cases, pathways were found on the HF/3-21G potential energy surface which consist of a series of valleys. (Valleys are paths along which the energy is a minimum with respect to any small displacement of the nuclei other than along the reaction coordinate.) Starting geometries corresponded to separated reactants or products, and R was varied incrementally. For each fixed value of R the remaining geometrical parameters were optimized within the chosen symmetry constraint and the second-derivative matrix was computed. If the second-derivative matrix was positive definite in the geometrical space exclusive of R, then the point was established as being on the valley floor and the reaction coordinate was incremented and the process repeated until a negative eigenvalue of the second-derivative matrix was obtained. This indicated that the valley being followed had ended; the precise end point is characterized by a zero eigenvalue. We have found two different modes for the termination of a valley. In the first, shown schematically in Figure 1a, a valley branches into a pair of equivalent valleys of lower symmetry, one of which is then followed. In the second, shown schematically in Figure 1b, the wall along the side of the valley has "eroded" away and the reaction pathway falls down the resulting hillside to a new valley. This new valley is then probed in the manner described above. The reaction forming diborane was examined by using a simpler path. At various fixed values of the B–B distance, the HF/6-31G* structures of H_2B--(H_2)--BH_2 were optimized within C_{2h} symmetry. Single-point MP2/6-31G* calculations were then performed to derive the appropriate pathway for dimerization. Detailed discussions of the three dimerization pathways are given in the individual sections.

The limitations of this "distinguished coordinate method" for studying reaction pathways have been pointed out by several authors.[17-19] The pathway is dependent on the choice of reaction coordinate, it need not include the transition structure, it can be discontinuous, and pathways for the forward and reverse directions of the same reaction can be different. This last phenomenon has been called chemical hysteresis,[20] and it is an artifact of the distinguished coordinate method.[21] Indeed, the second mode for the end of a valley, as described above, wherein there is a discontinuity in the pathway, will lead to "chemical hysteresis": there is no path from the lower valley to the upper one whereas the opposite is true. Despite these shortcomings, paths constructed by using the distinguished coordinate method can be informative. In addition, this is, to our knowledge, the first ab initio study where the calculation of the second-derivative matrix has been used to characterize the points along a reaction path.

All computations were performed using an extended version of the GAUSSIAN-80 program system.[22]

Discussion

Li_2H_2. Both the head-to-tail linear dimer, LiH–LiH, and the cyclic D_{2h}, Li--$(H)_2$--Li, forms of the lithium hydride dimer are substantially bound relative to two separated monomers, and the cyclic dimer is 21.6 kcal mol^{-1} lower in energy (MP4/6-31G**//HF/6-31G*). The dimerization energies to D_{2h} Li_2H_2, 46.2 kcal mol^{-1} (HF/6-31G**) and 47.8 kcal mol^{-1} (MP4/6-31G**), are in good accord with those of Ahlrichs.[23] His computations with a large basis of s and p functions gave a binding energy of 47.3 kcal mol^{-1} at the Hartree–Fock level and 48.3 kcal mol^{-1} with inclusion of electron correlation via the CEPA method. Ihle and Wu's experimental determination of the atomization

(15) DeFrees, D. J.; Levi, B. A.; Pollack, S. K.; Hehre, W. J.; Binkley, J. S.; Pople, J. A. *J. Am. Chem. Soc.* **1979**, *101*, 4085; **1980**, *102*, 2513.
(16) Hout, R. F.; Levi, B. A.; Hehre, W. J. *J. Comput. Chem.* **1982**, *3*, 234.
(17) Williams, I. H.; Maggiora, G. M. *J. Mol. Struct.* **1982**, *89*, 369.
(18) Müller, K. *Angew. Chem., Int. Ed. Engl.* **1980**, *19*, 1.
(19) Halgren, T. A.; Lipscomb, W. N. *Chem. Phys. Lett.* **1977**, *49*, 225.
(20) Dewar, M. J. S.; Kirschner, S. *J. Am. Chem. Soc.* **1971**, *93*, 4292.
(21) Dillon, P. W.; Underwood, G. R. *J. Am. Chem. Soc.* **1977**, *99*, 2435.
(22) Binkley, J. S.; Whiteside, R. A.; Krishnan, R.; Seeger, R.; DeFrees, D. J.; Schlegel, H. B.; Topiol, S.; Kahn, L. R.; Pople, J. A. *QCPE* **1981**, *13*, 406.
(23) (a) Ahlrichs, R. *Theor. Chim. Acta* **1974**, *35*, 59. Also see: (b) Kato, H.; Hirao, K.; Akagi, K. *Inorg. Chem.* **1981**, *20*, 3659. (c) Charkin, O. P.; Zjubin, A. S.; Gorbick, A. A. *Annu. Rep. Mendeleev's Inst. Chem. Tech.* **1984**, *134*, 13. (d) Zjubin, A. S.; Gorbick, A. A.; Charkin, O. P. *Zh. Strukt. Khim.* **1985**, *26*, 31. (e) Sukhanov, L. P.; Boldyrev, A. I.; Charkin, O. P. *Koord. Khim.* **1983**, *9*, 476.

TABLE VI: Ab Initio Thermochemistry for the Association Reactions[a]

dimer	$\Delta E°_{HF}$[b]	$\Delta E°_{corr}$[c]	$\Delta E°_{ZP}$[d]	$\Delta H°_0$	$\Delta H°_{298}$	$-T\Delta S°_{298}$	$\Delta G°_{298}$
Li--$(H)_2$--Li	−46.2	−1.6	+3.4	−44.4	−45.9	+8.9	−37.0
Li--$(H)_2$--BeH	−40.4	−5.7	+3.9	−42.2	−43.6	+8.3	−35.3
Li--$(H)_3$--BH	−49.9	−14.4	+5.9	−58.4	−60.1	+9.5	−50.6
HBe--$(H)_2$--BeH	−24.3	−8.9	+4.1	−29.1	−30.5	+8.6	−21.9
HBe--$(H)_3$--BH	−31.6	−18.4	+6.0	−44.0	−45.7	+9.5	−36.2
H_2B--$(H)_2$--BH_2	−21.4	−19.6	+7.1	−33.9	−36.0	+10.4	−25.6

[a] In kcal mol^{-1}. [b] 6-31G** basis set. See Table V. [c] MP4/6-31G** level. See Table V. [d] Computed from the data in Table III.

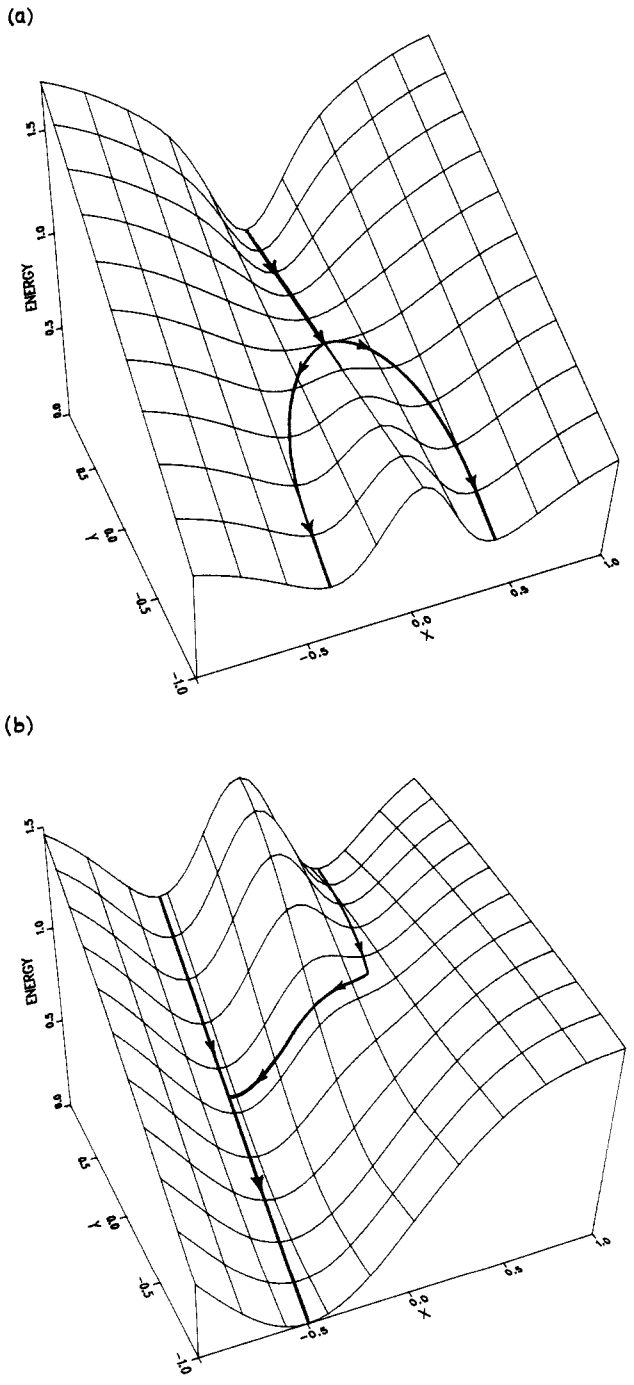

Figure 1. Potential surfaces showing two modes for the termination of a valley: (a) The valley branches into a pair of equivalent valleys. (b) The valley runs out onto the side of a hill.

energy of Li_2H_2,[5] 164 ± 8 kcal mol^{-1}, combined with the heats of formation at 0 K for Li, H, and LiH[24] gives a dimerization energy of 52 ± 8 kcal mol^{-1} for the lithium hydride dimer.[25]

(24) Stull, D. R.; Prophet, H. *JANAF Thermochemical Tables*, 2nd ed.; U.S. Government Printing Office: Washington, DC, 1971.

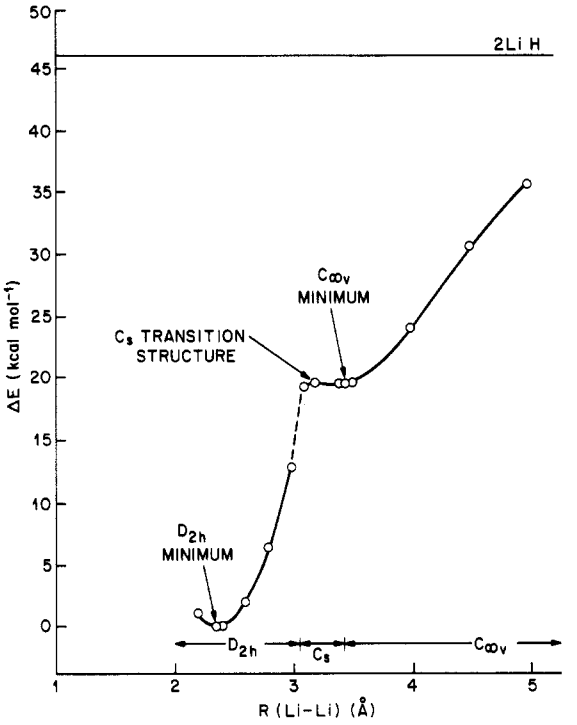

Figure 2. HF/3-21G potential curve for the dimerization of lithium hydride. This curve was constructed by following valleys on the potential surface beginning at R = 5 Å.

Second-derivative calculations with all three basis sets confirm that the cyclic dimer is a minimum on the potential energy surface. The linear dimer is not a minimum at the simplest STO-3G level of theory and has a degenerate pair of imaginary frequencies with π symmetry, indicating energy lowering on movement of the hydrogens off the Li–Li axis. However, the linear dimer is found to be a minimum at the higher 3-21G and 6-31G* levels. The inclusion of electron correlation at the MP2(Full)/6-31G* level does not change the qualitative result: the second-derivative matrix for the linear dimer has no negative eigenvalues, and LiH–LiH is thus a minimum on the potential energy surface.

The HF/3-21G potential energy of two approaching LiH molecules is shown in Figure 2. The dimerization path was generated by following valleys on the surface as the reaction coordinate (the Li–Li distance) was decreased from an initial value of 5 Å. At longer distances, electrostatic interaction between monomer dipoles dominates and linear forms, LiH--LiH, are the most stable. As the molecules approach further, the energy decreases until the $C_{\infty v}$ local minimum at a lithium–lithium distance of 3.445 Å is reached. At lower values of R the energy increases, and by 3.4 Å the $C_{\infty v}$ valley has branched into a pair of equivalent valleys of C_s symmetry. If either of these C_s valleys is followed by further reducing R, the energy of the system increases until a saddle point is encountered at a Li–Li distance of 3.255 Å (**1**). The energy of this saddle point is only 0.1 kcal mol^{-1} above the

(25) Note, however, that Ihle and Wu[5] report an atomization energy for LiH_2 which appears to be too large. Only a van der Waals complex was found at higher levels of theory. Hobza, P.; Schleyer, P. v. R. *Chem. Phys. Lett.* **1984**, *105*, 830. Garcia-Prieto, J.; Feng, W. L.; Novaro, O. *Chem. Phys. Lett.* **1985**, *119*, 128.

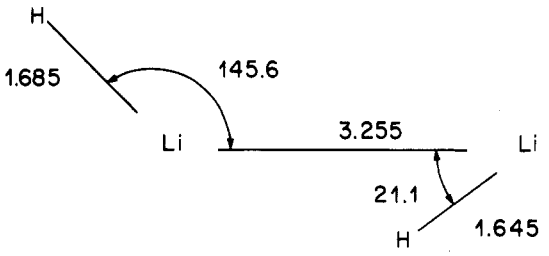

1

linear minimum despite a large change in geometry. The energies along both C_s valleys decrease until R(Li–Li) = 3.0 Å, where they end with a zero frequency (Figure 1b). There is a discontinuity in the curve, and at the bottom of the resultant hillside is a D_{2h} valley which is followed to the D_{2h} minimum at R = 2.364 Å. At no point along the reaction path is the energy greater than that of two noninteracting monomers. Hence, the dimerization occurs without overall activation. The discontinuity in the curve is an artifact of the use of a reaction coordinate; a different path results if we start at the cyclic minimum and pull the lithiums apart. The D_{2h} valley is followed until the lithiums are 3.15 Å apart where a branch into two equivalent C_{2h} valleys is encountered. The C_{2h} valleys themselves branch at approximately 3.3 Å into the incoming C_s valleys. From this point on out, the incoming and outgoing paths are the same.

$LiBeH_3$. Isomers containing one (LiH--BeH_2), two (Li--$(H)_2$--BeH), and three (Li--$(H)_3$--Be) bridging hydrogens corresponding to corner, edge, and face attachments of Li^+ to planar BeH_3^- have been compared previously.[2,26] At each theoretical level employed here (Table V) the dibridged isomer is the most stable, followed by the tribridged and the monobridged forms in that order. With our most sophisticated model (MP4/6-31G**//HF/6-31G*), the corresponding LiH + BeH_2 association energies are 46.1, 34.2, and 23.1 kcal mol^{-1}, respectively. Charkin's group studied the same isomers with several basis sets and also at correlated levels.[26] Their binding energies and geometries are in good accord with our results. In addition, their optimized structures agree well with the 3-21G geometries.

Whereas the isomers with two and with three bridging hydrogens are found via analytical evaluation of the second-derivative matrix to be minima on the potential energy surface, the singly bridged isomer, LiH--BeH_2, is unstable with respect to both in-plane and out-of-plane motions of the lithium relative to BeH_3. Figure 3 shows the HF/3-21G energy as a function of the Li--Be--H angle for the out-of-plane motion; all three isomers are included on the path which was generated by energy minimization within C_s symmetry. Full optimization and a second-derivative calculation give **2** as the HF/3-21G transition structure for the transformation Li--(H_3)--Be → Li--$(H)_2$--BeH. The activation energy for this process is computed to be only 0.2 kcal mol^{-1} (HF/3-21G//HF/3-21G) and 0.04 kcal mol^{-1} with the HF/6-31G*//HF/6-31G* model. Structure **2** is also the transition structure for scrambling of the terminal and bridging hydrogens in the dibridged isomer, with the tribridged form as a possible intermediate in which all three hydrogens are equivalent. Inclusion of electron correlation effects at the MP2(Full)/6-31G* level changes this picture somewhat as at this level the tribridged isomer itself has a negative eigenvalue of the force constant matrix. This

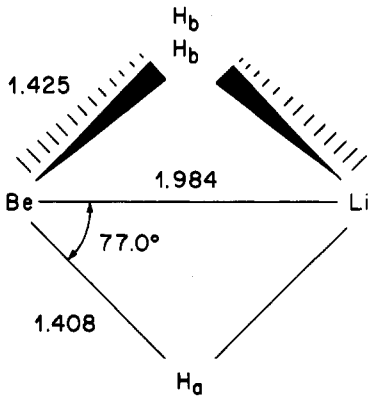

< Li Be H_{bb} = 39.4°

< H_b Be H_b = 108.8°

2

indicates that the tribridged isomer itself is the transition structure for hydrogen scrambling and, in fact, may be the only true transition structure on the potential energy surface. The MP4/6-31G**//HF/6-31G* barrier to scrambling is roughly 12 kcal mol^{-1}, the difference in stability of dibridged and tribridged isomers.

Boldyrev, Sukhanov, and Charkin have computed reaction paths leading from LiH and BeH_2 to each of the three dimer structures.[27] In each case the dimerization occurs without overall activation.

$LiBH_4$. The C_{3v} isomer, Li--$(H)_3$--BH, with three bridging hydrogens is more stable than the C_{2v} dibridged isomer, Li--$(H)_2$--BH_2, at all levels of theory (Table V). The energy difference is 6.2 kcal mol^{-1} (MP4/6-31G**//HF/6-31G*). The binding energy of Li--$(H)_3$--BH, 64.3 kcal mol^{-1}, is the largest of the six association complexes which we have studied.

A second-derivative calculation confirms Li--$(H)_3$--BH to be a minimum on the potential energy surface and that Li--$(H)_2$--BH_2 is a saddle point characterized by a single imaginary frequency. Examination of the normal coordinate giving rise to the imaginary frequency leads to the conclusion that the C_{2v} form is the transition structure for interconversion of equivalent C_{3v} molecules. This hydrogen scrambling reaction can be viewed as the movement of Li^+ from one face of a BH_4^- tetrahedron to another equivalent face with the highest energy occuring when the Li^+ is over an edge of the tetrahedron. The MP4/6-31G** activation energy for this process is only 6.2 kcal mol^{-1}. Boldyrev et al.,[28] using a large s–p basis set, obtained geometries similar to ours at the 3-21G level. In addition, they computed a number of points on the potential energy surface relevant to the hydrogen scrambling reaction which revealed that edge lithiated borohydride, Li--$(H)_2$--BH_2, is the transition structure. Single-point Hartree–Fock computations carried out with a somewhat larger s–p basis, augmented by polarization functions, gave an activation energy of 4.6 kcal mol^{-1} for the process. Bonaccorsi et al.[29] examined $LiBH_4$, $NaBH_4$, $LiAlH_4$, and $NaAlH_4$ with STO-3G and double-ζ basis sets. The results they obtained for lithium borohydride agree with those of Boldyrev et al.[28]

Be_2H_4. The first of the three isomers of Be_2H_4 which we have investigated, HBeH--BeH_2, is a T-shaped molecule, only slightly bound relative to a pair of noninteracting BeH_2 molecules, whose structure and energy are consistent with a quadrapolar interaction between the monomers. This form is a saddle point on the full

(26) (a) Boldyrev, A. I.; Charkin, O. P.; Rambidi, N. E.; Andeev, V. I. *Chem. Phys. Lett.* **1976**, *44*, 20. (b) Zakzhevskii, V. G.; Boldyrev, A. I.; Charkin, O. P.; Bozhenko, K. V.; Klimenko, N. M. *Zh. Neorg. Khim.* **1979**, *24*, 1764. (c) Smolyar, A. E.; Zyubin, A. S.; Khaikina, E. A.; Charkin, O. P. *Zh. Neorg. Khim.* **1980**, *25*, 307. (d) Sukhanov, L. P.; Boldyrev, A. I.; Charkin, O. P. *Koord. Khim.* **1981**, *6*, 803. (e) Zjubin, A. S.; Chaban, G. M.; Gorbik, A. A.; Charkin, O. P. *Zh. Strukt. Khim.* **1985**, *26*, 12 and ref 23c. (f) Cimiraglia, R.; Persico, M.; Tomasi, J.; Charkin, O. P. *J. Comput. Chem.* **1984**, *5*, 263. (g) Sukhanov, L. P.; Boldyrev, A. I. *Zh. fiz. Khim.* **1984**, *58*, 654. (h) Boldyrev, A. I.; Sukhanov, L. P.; Charkin, O. P. *Koord. Khim.* **1982**, *8*, 430. (i) Sukhanov, L. P.; Boldyrev, A. I.; Charkin, O. P. *Chem. Phys. Lett.* **1983**, *97*, 373. (j) Wurthein, E.-U.; Krogh-Jespersen, M.-B.; Schleyer, P. v. R. *Inorg. Chem.* **1981**, *20*, 3663.

(27) Boldyrev, A. I.; Sukhanov, L. P.; Charkin, O. P. *Chem. Phys.* **1980**, *51*, 205. Also see ref 26.

(28) (a) Boldyrev, A. I.; Charkin, O. P.; Rambidi, N. E.; Avdeev, V. I. *Chem. Phys. Lett.* **1976**, *44*, 20. (b) Charkin, O. P.; Mysaev, D. G.; Klimenko, N. M. *Koord. Khim.* **1985**, *11*, 728. (c) Kello, V.; Urban, M.; Boldyrev, A. I. *Chem. Phys. Lett.* **1984**, *106*, 455. Also see ref 23a.

(29) Bonaccorsi, R.; Scrocco, E.; Tomasi, J. *Theor. Chim. Acta* **1979**, *52*, 113.

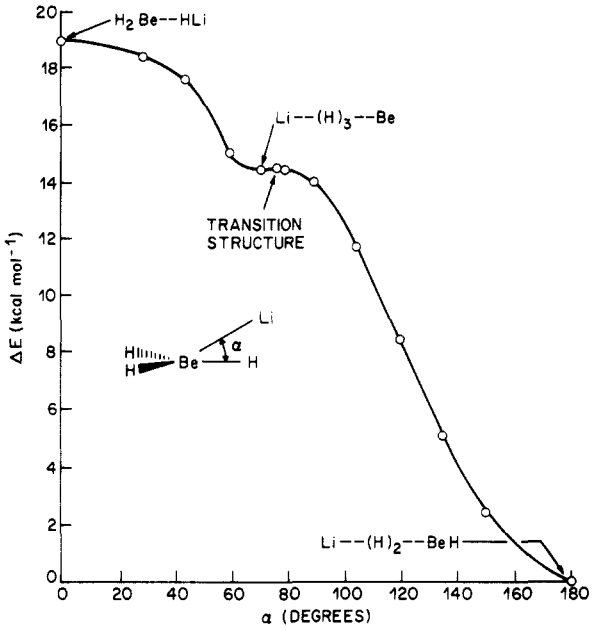

Figure 3. HF/3-21G potential curve for the interconversion of $LiBeH_3$ isomers. This curve was constructed by performing HF/3-21G geometry optimizations within C_s symmetry with α fixed. The tribridged isomer, however, becomes the transition structure for hydrogen scrambling at higher levels of theory (see text).

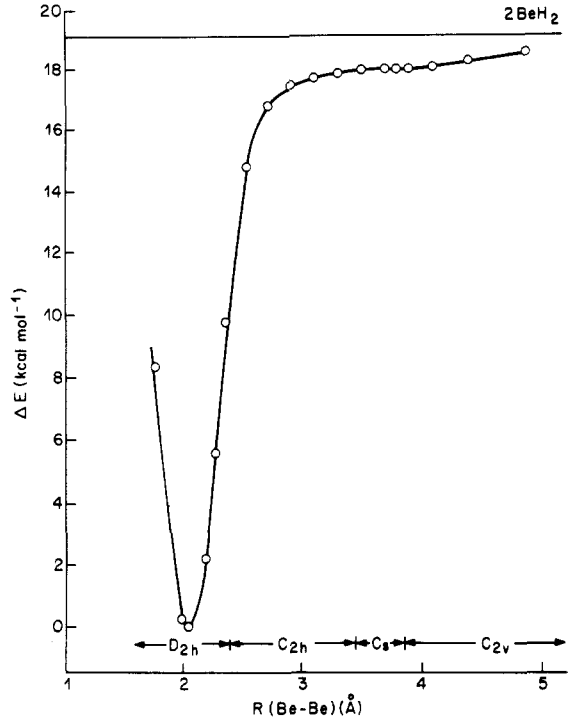

Figure 4. HF/3-21G potential curve for the dimerization of beryllium hydride. This curve was constructed by following valleys on the potential surface.

Be_2H_4 potential energy surface as has also been found in previous studies.[26i,f,30] The second isomer, HBe--$(H)_2$--BeH, is the lowest energy minimum. Our computed structure is in essential agreement with that of Ahlrichs,[31] who used several large s–p basis sets and the independent electron pair approximation (IEPA) to estimate the correlation energy. His estimate for the BeH_2 dimerization energy, 31 kcal mol^{-1}, is in good agreement with our value, 33.2 kcal mol^{-1} (MP4/6-31G**//HF/6-31G*). The large variation of the Hartree–Fock dimerization energy with changes in the basis set reported by Ahlrichs (e.g., 13.4, 9.8, and 21.6 kcal mol^{-1}) is not reflected by our calculations nor of those by Charkin et al.[30b] The third isomer, HBe--$(H)_3$--Be, although a potential minimum, is unbound with respect to dissociation into two BeH_2 monomers at all Hartree–Fock levels. However, the inclusion of correlation results in a stabilization of the dimer relative to the monomers, so that at the MP4/6-31G** level this triply bridged structure is bound by 11.2 kcal mol^{-1} and is 9.6 kcal mol^{-1} lower in energy than the singly bridged dimer.

The transition structure for scrambling of the bridge and terminal hydrogens in HBe--$(H)_2$--BeH is the singly bridged isomer. The normal coordinate associated with the imaginary frequency (**3**) can be viewed as a rotation of a BeH_3^- fragment

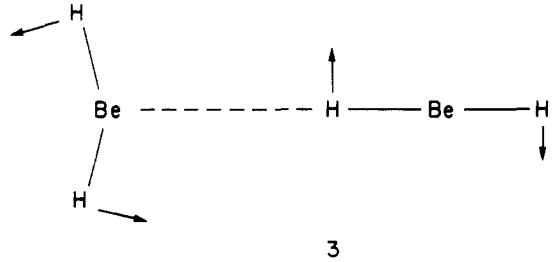

3

relative to a fixed BeH^+ fragment. At the MP4/6-31G** level, the activation energy for hydrogen scrambling is 31.6 kcal mol^{-1}.

The HF/3-21G potential energy of the system as a function of the beryllium–beryllium distance is presented in Figure 4. The pathway was defined by following valleys on the potential surface as the beryllium–beryllium distance was varied. Unlike the LiH dimerization, the path is continuous with no chemical hysteresis effects. At large monomer–monomer separations the T-shaped structure with a single bridging hydrogen is the most stable. As the beryllium atoms are brought closer together, a valley with C_{2v} symmetry is followed until it ends at R(Be–Be) = 3.84 Å. (Compare this with a beryllium–beryllium distance of 3.77 Å at the C_{2v} minimum.) Here the valley branches into two equivalent valleys of C_s symmetry as structures with the bridging hydrogen off the Be–Be axis become stable. Starting at the minimum for the dibridged isomer HBe--$(H)_2$--BeH, and separating the two beryllium atoms, a valley with D_{2h} symmetry is followed until R(Be–Be) = 2.36 Å where it splits into two valleys of C_{2h} symmetry. In this lower symmetry, the bridging hydrogens are not equally shared between the two beryllium atoms: each is associated with a particular Be. The C_{2h} valley is followed until a Be–Be separation of 3.44 Å at which point it branches into two equivalent valleys of C_s symmetry, identical with the incoming C_s valleys. There is no activation energy for the overall dimerization reaction at the HF/3-21G level of theory. Comparison of Figure 4 with Figure 2 for the interaction of a pair of lithium hydrides makes the rapid falloff with distance of the interaction of two quadrupoles relative to two dipoles readily apparent.

$BeBH_5$. Three isomers of $BeBH_5$, containing one (HBeH--BH_3), two (HBe--$(H)_2$--BH_2), and three (HBe--$(H)_3$--BH) bridging hydrogens, have been examined. The first is only slightly bound relative to BeH_2 + BH_3 and has a degenerate pair of imaginary frequencies at the HF/6-31G* level. The C_{2v} dibridged and C_{3v} tribridged structures, both of which are minima on the potential surface at that level, are very close in energy, with the latter form being more stable at every theoretical level in our study except HF/3-21G//HF/3-21G. A similar basis set effect was noted by Kirillov et al.[32] At our final MP4/6-31G**//HF/6-31G* theoretical level the C_{3v} isomer is 5.4 kcal mol^{-1} more stable than the C_{2v} form. Ahlrichs[33] found the tribridged structure to be the more stable by 6.8 kcal mol^{-1} using a large s–p Gaussian

(30) (a) Solomnik, V. G.; Sayonova, I. G.; Krasnov, K. S. *Theor. Exp. Chem. (Engl. Transl.)* **1980**, *16*, 571. (b) Sukhanov, L. P.; Boldyrev, A. I.; Charkin, O. P. *Koord. Khim.* **1983**, *9*, 762.
(31) Ahlrichs, R. *Theor. Chim. Acta* **1970**, *17*, 348.
(32) (a) Kirillov, Y. B.; Boldyrev, A. I.; Klimenko, N. M. *Russ. J. Coord. Chem.* **1980**, *6*, 742. (b) Kirillov, Y. B.; Klimenko, N. M.; Zakzhevskii, V. G. *Zh. Strukt. Khim.* **1983**, *24*, 469.
(33) Ahlrichs, R. *Chem. Phys. Lett.* **1973**, *19*, 174.

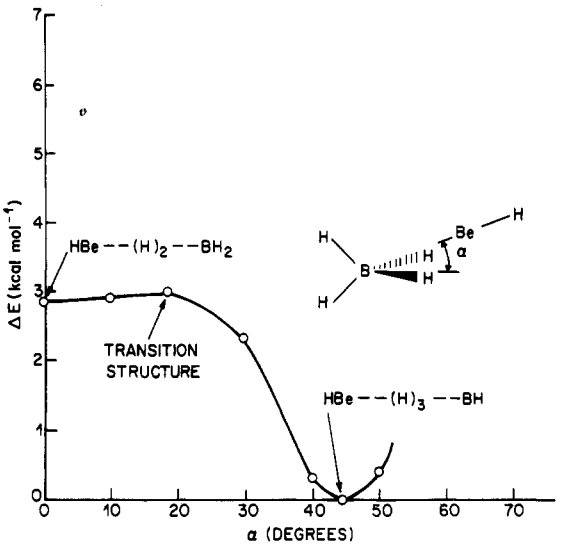

Figure 5. HF/3-21G potential curve for the interconversion of $BeBH_5$ isomers. This curve was constructed by performing HF/3-21G geometry optimizations within C_2 symmetry with α fixed. The dibridged isomer, however, becomes the transition structure at higher levels of theory (see text).

lobe function basis and the IEPA-PNO method for estimating the correlation energy.

Figure 5 shows the energy along a reaction path connecting the dibridged and tribridged isomers. The HF/6-31G* path was computed by optimizing the geometry within C_s symmetry at various fixed values of the angle α, as shown in the figure. A striking feature of the curve is its flatness, particularly in the region of the C_{2v} minimum. At this level the saddle point lies just 0.14 kcal mol^{-1} above HBe--$(H)_2$--BH_2 and is the transition structure for a reaction which scrambles four of the five hydrogens as well as interconverting the isomers. (We could not locate a low-energy pathway at the HF/3-21G level which would bring about scrambling of the fifth hydrogen.) In fact, further optimization and vibrational analysis at the MP2(Full)/6-31G* level for the dibridged structure shows the presence of a negative eigenvalue of the force constant matrix, indicating that this structure is a saddle point rather than a minimum. This agrees with Ahlrichs' conclusion[33] that the tribridged form is the only minimum.

B_2H_6. Diborane is the only one of the six systems for which there is experimental structural data. Molecules containing one, two, and three bridging hydrogen atoms were studied. All structures with one or three such linkages either dissociated without activation to two BH_3 monomers or rearranged without activation to the dibridged molecule. The dimerization energy to H_2B--$(H)_2$--BH_2 computed at the MP4/6-31G**//HF/6-31G* level, 41.0 kcal mol^{-1}, is in good accord with the results of Redman, Purvis, and Bartlett,[34] who used Møller–Plesset theory to partial sixth order with a basis set somewhat larger than ours, of Taylor and Hall,[35] who included all valence singles and doubles CI from a generalized molecular orbital wave function, and of Frisch, Krishnan and Pople,[36] who used fourth-order perturbation theory, MP4/6-31G*. Our ab initio estimate for the enthalpy of dimerization at 298 K of −36.0 kcal mol^{-1} (Table VI) is in perfect accord with most of the experimental determinations[34] which are in the range −36 ± 3 kcal mol^{-1}.

Figure 6 shows two potential energy curves for the dimerization of BH_3 to form H_2B--$(H)_2$--BH_2. The lower path was generated by optimizing B_2H_6 within C_{2h} symmetry at the HF/6-31G* level with various fixed B–B distances. Single-point calculations along the resultant path at the MP2/6-31G* level of theory gave the upper potential curve. The three Hartree–Fock stationary points

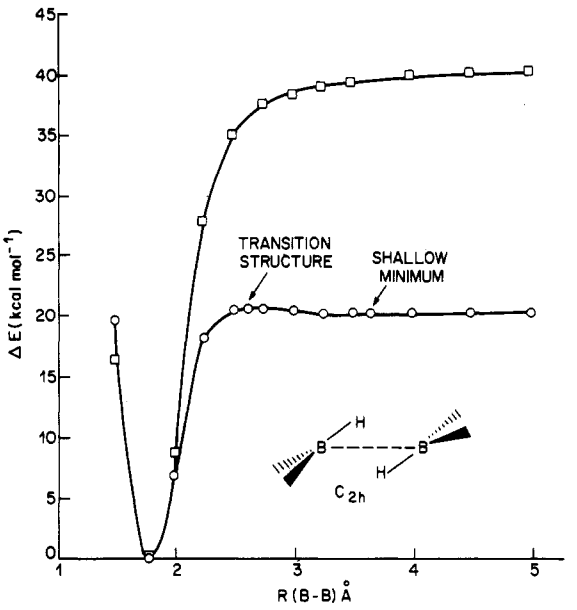

Figure 6. Potential curves for the dimerization of boron hydride. The lower curve (○) was constructed by performing HF/6-31G* geometry optimizations of B_2H_6 within C_{2h} symmetry with R(B–B) fixed. The upper curve (□) was constructed by performing MP2/6-31G* single-point calculations using the structures determined along the C_{2h} HF/6-31G* pathway.

are the D_{2h} minimum at R(B–B) = 1.778 Å, a shallow minimum at R(B-B) = 3.645 Å, only 0.1 kcal mol^{-1} below $2BH_3$, and the transition structure connecting the two minima at R(B–B) = 2.623 Å with an energy 0.5 kcal mol^{-1} above that of the weakly bound minimum. The HF/STO-3G and HF/3-21G curves are similar. An early study by Dixon et al.[37] of the C_{2h} path using the PRDDO method and a minimal basis set SCF + all singles and doubles CI calculation gave qualitatively similar curves. Their SCF–CI transition state lay 2.6 kcal mol^{-1} above separated BH_3 molecules at a B–B distance of 3.0 Å. The MP2/6-31G*//HF/6-31G* potential energy curve has only one stationary point corresponding to the ground-state diborane. The inclusion of correlation energy thus gave not only a much larger dimerization energy but also a monotonic decrease in energy as the constituent monomers approach each other. An experimental investigation of the kinetics of this reaction resulted in an estimate of 0 ± 2 kcal mol^{-1} for the activation energy along with the statement that it is "probably negative".[38]

Conclusions

Ab initio molecular orbital theory at the Hartree–Fock and Møller–Plesset (through complete fourth order) levels was used to investigate the six binary association complexes formed from lithium hydride, beryllium hydride, and boron hydride (borane). In answer to the five questions posed in the introduction, we discovered the following:

1. The 6-31G*//6-31G* binding energies compared well with the previously published 6-31G*//STO-3G results.[2] Even in those instances where there is a large structural change in going from the STO-3G to the 6-31G* basis, the binding energies agree to within a few tenths of a kilocalorie. This is due in part to the flatness of the potential surfaces; large changes in geometry can lead to small changes in energy.

2. The addition of p polarization functions to the hydrogen basis (to form 6-31G**) has little effect on either the absolute or relative energies of these complexes. There is no clear trend as a function of the number of bridging hydrogens; however, the change in binding due to the addition of p functions increases

(34) Redman, L. T.; Purvis, G. D.; Bartlett, R. J. *J. Am. Chem. Soc.* **1979**, *101*, 2856.
(35) Taylor, T. E.; Hall, M. *J. Am. Chem. Soc.* **1980**, *102*, 6136.
(36) (a) Frisch, M. J.; Krishnan, R.; Pople, J. A. *Chem. Phys. Lett.* **1980**, *76*, 66. (b) Ortiz, J. V.; Lipscomb, W. N. *Chem. Phys. Lett.* **1983**, *103*, 59.
(37) (a) Dixon, D. A.; Pepperberg, I. M.; Lipscomb, W. N. *J. Am. Chem. Soc.* **1975**, *96*, 1325. (b) For an MNDO study, see: Ip, W.-K.; Li, W.-K. *Croat. Chem. Acta* **1984**, *57*, 1451.
(38) Mappes, G. W.; Fuidmann, S. A.; Fehlner, T. P. *J. Phys. Chem.* **1970**, *74*, 3307.

roughly with the number of electrons.

3. Several of the stationary points were found to be saddle points (one imaginary frequency) or double saddles (two imaginary frequencies). In several instances the nature of the stationary point changed with basis set or with the inclusion of electron correlation, another consequence of the general flatness of these potential surfaces.

4. In all cases the inclusion of electron correlation corrections leads to an increase in the association energies. This effect is small for Li--$(H)_2$--Li but increases markedly as the number of electrons in the complex increases. The correlation effects are additive to within ±2 kcal mol^{-1} for the most stable isomers when the following values are used: Li, 1 kcal mol^{-1}; Be, 5 kcal mol^{-1}; B, 11 kcal mol^{-1}. The correlation contribution is greater when the number of bridging hydrogens is greater. Although correlation does not alter the relative isomers stabilities, it does lead to significant binding in HBe--$(H)_3$--Be which is unbound at HF/6-31G**//HF/6-31G*.

5. Dimerization reactions of LiH and of BeH_2 proceed without activation with the HF/3-21G theoretical model. The formation of diborane from $2BH_3$ also proceeds without activation on the MP2/6-31G* potential energy surface. These results are expected since no bond-breaking or repulsive interactions are involved.

Acknowledgment. This work was supported by the National Science Foundation under Grant CHE 81-01061-01 and by the Fonds der Chemischen Industrie and was facilitated by an Alexander von Humboldt award to John A. Pople.

Registry No. Li_2H_2, 12435-82-4; $LiBeH_3$, 25282-11-5; $LiBH_4$, 16949-15-8; Be_2H_4, 29860-66-0; $BeBH_5$, 39357-33-0; B_2H_6, 19287-45-7.

Test of the Hubbard–Onsager Dielectric Friction Theory of Ion Mobility in Nonaqueous Solvents. 1. Ion-Size Effect

K. Ibuki and M. Nakahara*

Department of Chemistry, Faculty of Science, Kyoto University, Kyoto 606, Japan *(Received: August 19, 1986; In Final Form: October 15, 1986)*

The Hubbard–Onsager (HO) dielectric friction theory was tested systematically for mobility of the alkali metal, halide, and tetraalkylammonium ions in four types of polar solvents at 25 °C; the solvents studied were water, alcohols (methanol, ethanol, and 1-propanol), amides (formamide and *N*-methylformamide), and dipolar aprotic solvents (acetone and acetonitrile). Instead of the conventional Walden product, we used the residual friction coefficient ($\Delta\zeta$) defined as the total friction coefficient minus the Stokes friction coefficient for slip. The experimental curve of $\Delta\zeta$ vs. ion radius is V-shaped in all solvents. The HO theory is successful in predicting the size dependence of $\Delta\zeta$ for the relatively small ions not only in the aprotic solvents but also in the other hydrogen-bonded solvents. However, the negative values of $\Delta\zeta$ observed for the medium-sized ions in the hydrogen-bonded solvents and the increase in $\Delta\zeta$ with increasing size of the tetraalkylammonium ions are not explained by the continuum theory.

Introduction

For a long time ordinary hydrodynamics has been applied to interpret the dynamic properties of ions in solution. Such a typical example is seen in the study of ion mobility and molecular diffusion where the Stokes–Einstein–Walden (SEW) framework based on the Navier–Stokes (NS) hydrodynamic equation of motion is prevalent. The NS hydrodynamic equation may be applicable to uncharged systems but, in principle, not to ionic systems of our interest. To overcome the fundamental limitations of ordinary hydrodynamics, Hubbard and Onsager[1,2] (HO) developed the dielectric friction theory and invented the epoch-making electrohydrodynamic equation for migrating ions; HO extended the NS hydrodynamic equation to ionic systems in a self-consistent manner by adapting the Debye dielectric relaxation theory to the flow system involving a charged sphere.

The apparent limitations of the SEW framework is often ascribed to the neglect of the liquid structure of solvent rather than to the neglect of the essential effect of the charge on an ion in the continuum model; the effect of the liquid structure on ion dynamics is to be discussed only after the effect of charge is properly taken into account as in the HO theory. In the treatment of ion dynamics in solution, now is the time to replace the classical SEW framework by a modern one due to the HO dielectric friction theory. For this reason an extensive test of the reliability of the HO theory is necessary. Since the experimental test of the HO theory has been confined to aqueous systems in the previous series of papers,[3-11] it is extended to nonaqueous systems in the present series. Such a test limited to aqueous systems is insufficient for an understanding of the general feature of the HO theory because of the well-known peculiarities of water. We must test the theory also in nonaqueous systems. The high precision and abundance of measured ionic conductances are of benefit to the stringent test of the general feature of the HO electrohydrodynamic equation of motion which is applicable to ion translation[1-11] and rotation[12,13] and electrolyte viscosity.[14]

It has been clearly shown in a previous paper[10] that the undue transformation of the limiting ionic conductance λ^0 into the conventional Walden product distorts and obscures the original meaning of λ^0. Instead, we have recommended the transformation

(1) Hubbard, J.; Onsager, L. *J. Chem. Phys.* **1977**, *67*, 4850.
(2) Hubbard, J. *J. Chem. Phys.* **1978**, *68*, 1649.
(3) Takisawa, N.; Osugi, J.; Nakahara, M. *J. Phys. Chem.* **1981**, *85*, 3582.
(4) Nakahara, M.; Török, T.; Takisawa, N.; Osugi, J. *J. Chem. Phys.* **1982**, *76*, 5145.
(5) Takisawa, N.; Osugi, J.; Nakahara, M. *J. Chem. Phys.* **1982**, *77*, 4717.
(6) (a) Takisawa, N.; Osugi, J.; Nakahara, M. *J. Chem. Phys.* **1983**, *78*, 2591. (b) Nakahara, M.; Takisawa, N.; Osugi, J. In *High Pressure in Science and Technology*, Homan, C.; MacCrown, R. K.; Whalley, E., Eds.; North Holland: New York, 1984; Part II, p 169.
(7) Nakahara, M.; Zenke, M.; Ueno, M.; Shimizu, K. *J. Chem. Phys.* **1985**, *83*, 280.
(8) Ibuki, K.; Nakahara, M. *J. Chem. Phys.* **1986**, *84*, 2776.
(9) Ibuki, K.; Nakahara, M. *J. Chem. Phys.* **1986**, *84*, 6979.
(10) Nakahara, M.; Ibuki, K. *J. Phys. Chem.* **1986**, *90*, 3026.
(11) Ibuki, K.; Nakahara, M. *J. Phys. Chem.* **1986**, *90*, 6362.
(12) Nakahara, M.; Ibuki, K. *J. Chem. Phys.* **1986**, *85*, 4654.
(13) Felderhof, B. U. *Mol. Phys.* **1983**, *48*, 1283.
(14) (a) Ibuki, K.; Nakahara, M. *J. Chem. Phys.* **1986**, *85*, 7312. (b) Ibuki, K.; Nakahara, M. *J. Chem. Phys.*, in press.

0022-3654/87/2091-1864$01.50/0